DyCSC: Modeling the Evolutionary Process of Dynamic Networks Based on Cluster Structure

Shanfan Zhang, Zhan Bu

Abstract

Temporal networks are an important type of network whose topological structure changes over time. Compared with methods on static networks, temporal network embedding (TNE) methods are facing three challenges: 1) it cannot describe the temporal dependence across network snapshots; 2) the node embedding in the latent space fails to indicate changes in the network topology; and 3) it cannot avoid a lot of redundant computation via parameter inheritance on a series of snapshots. To this end, we propose a novel temporal network embedding method named Dynamic Cluster Structure Constraint model (*DyCSC*), whose core idea is to capture the evolution of temporal networks by imposing a temporal constraint on the tendency of the nodes in the network to a given number of clusters. It not only generates low-dimensional embedding vectors for nodes but also preserves the dynamic nonlinear features of temporal networks. Experimental results on multiple realworld datasets have demonstrated the superiority of *DyCSC* for temporal graph embedding, as it consistently outperforms competing methods by significant margins in multiple temporal link prediction tasks. Moreover, the ablation study further validates the effectiveness of the proposed temporal constraint.

Introduction

Temporal graphs are mainly defined in two ways: (1) discrete temporal graphs, which are a collection of evolving graph snapshots at multiple discrete time steps; and (2) continuous temporal graphs, which update too frequently to be represented well by snapshots and are instead denoted as graph streams[8]. In this paper, we will focus mainly on the former.

Research motivation. The set of approaches most relevant to our work is the recurrent learning scheme that integrates graph neural networks with the recurrent architecture, whereby the former captures graph information and the latter handles temporal dynamism by maintaining a hidden state to summarize historical snapshots(e.g., VGRNN[3]). However, they have the following two drawbacks

- They focus too much on updating model parameters while neglecting to capture the variation in network topology from the perspective of node representation vectors, i.e., existing models lack necessary and effective connections between representation vectors generated for the same node at different moments. The way to alleviate this defect is mainly to impose conditional constraints on the model by adding regular terms to the two embedding vectors generated by the model to the same node in the network at two adjacent moments because it's natural to assume that a network will evolve smoothly over time, instead of being totally rebuilt in each time step. For example, *DynamicTriad*[12] defines the temporal smoothness by minimizing the Euclidean distance between embedding vectors in adjacent time steps, i.e., $\mathcal{L}_{smooth} = \sum_{i=1}^{|v|} \left\|\mathbf{u}_i^t - \mathbf{u}_i^{t-1}\right\|_2^2, t > 1$.
- They ignores to dynamically capture the cluster structure in the network which characterizes the local aggregation characteristics and reflects the distribution inhomogeneity of connected links in the network. Figure 1 simulates a dynamic graph with three communities where a node (red colored node) transfers from one community into another in two time steps, and simultaneously accompanied by drastic changes in its neighbor nodes. We can clearly observe that the community structure in the network is constantly changing as the network continues to evolve. However, as shown in Fig. 1, the targeted red node bias towards individual communities should be gradually changed, meaning that it does not suddenly move from one community to another.

This paper will strive to explore how to use the cluster structure of a dynamic network to obtain high-quality dynamic node embeddings that can accurately its dynamic changing process. Specifically, our model will be based on the following four assumptions:

1) The more similar the representation vectors of the two nodes, the greater the probability of forming an edge between them;

2) The more similar the tendency of two nodes to various clusters, the more likely the probability of forming an edge between them;

3) At adjacent times, the tendency of the same node to different clusters should change little, that is, the change of network cluster structure should be a gradual process;

4) The topology of the next moment of the network should be the result of the topology of each moment in the previous time, that is, the relationship between two nodes in the network can be determined by their relationship in the previous time.

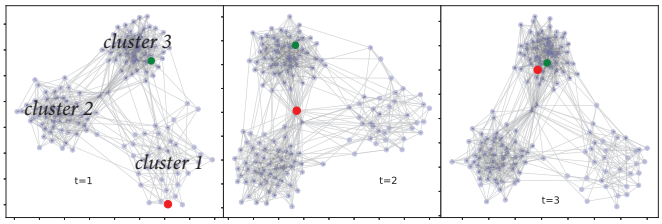

Figure 1: Evolution of simulated graph topology through time[3].

Contribution. To summarize, we have made the following innovative contributions in this work:

1. We innovatively introduce the cluster structure into the dynamic node embedding model, and the time constraint imposed accordingly makes *DyCSC* more relevant to the node embedding generated by the network at adjacent moments, thus obtaining better interpretation.
2. Different from the prior approaches which rely on RNN output during the GNN stage of embedding or merely incorporate GNNs into the RNN architecture to force the models to work continuously, we calculate the structural similarity between nodes at each moment and store them in a separate memory network which will be read out as historical information when predicting the network at the next moment. Such an architecture not only greatly reduces the number of parameters that *DyCSC* needs to train, but also has the most important advantage that only one node embedding operation is required for the network at each moment since the results can be reused.
3. We demonstrate that for temporal link prediction and detection, the simple framework we propose is equally or more accurate and precise than state-ofthe-art temporal graph autoencoder models. *DyCSC* attains about equal metrics to the state-of-the-art in inductive link detection tests, and higher area under the curve and average precision scores by 2% in transductive link prediction tests.

The rest of this work is organized as follows: Section II discusses the problem definition and defines our key terms. Section III explains the *DyCSC* framework in detail. IV compares the performance of *DyCSC* against a diverse set of competing graph embedding methods. Finally, we conclude this paper with a brief discussion in Section V.

PRELIMINARIES AND PROBLEM DEFINITION

Temporal Network

A discrete temporal graph $\mathcal{G} = \{\mathcal{G}_1, \mathcal{G}_2, \cdots, \mathcal{G}_T\}$ is defined as a series of graphs $\mathcal{G}_t = \{\mathcal{V}_t, \mathcal{A}_t\}$, which we refer to as snapshots, representing the state of a network at time t. Here, T is the number of snapshots, $\mathcal{V}_t$ and $\mathcal{A}_t$ denotes the set of all nodes which appear in the network and relationships between nodes at time t, respectively.

Problem Definition

Given the sequence of snapshots $\mathcal{G}$, we need to obtain the representations of every node $\mathbf{u}$ for each snapshot t in a low-dimensional vector space ($\mathbf{d}$-dimensional) as $\left\{\mathbf{h}_\mathbf{u}^1, \mathbf{h}_\mathbf{u}^2, \cdots, \mathbf{h}_\mathbf{u}^T\right\}$, where $\mathbf{h}_\mathbf{u}^t \in \mathbb{R}^\mathbf{d}$ is the embedding of node $\mathbf{u}$ at time t and $\mathbf{d}$ represents the dimension of the embedding space. We also denote $\mathbf{H}^t \in \mathbb{R}^{N\times\mathbf{d}}$ as the embedding matrix of nodes in the snapshot t, N is the number of nodes. *DyCSC* is reflected by a mapping function: $\mathbf{H}^t = \mathcal{F}\left(\mathcal{A}^{\leq t}\right)$, where $\mathcal{A}^{\leq t}$ denotes some adjacency matrices at time less than t, such that $\mathbf{H}^t$ is able to capture the temporal evolution of the network and be used to predict $\mathbf{H}^{t+1}$. More specifically, we wish to predict the structure of $\mathcal{A}^{t+1}$ based on the historical structure $\mathcal{A}^{\leq t}$. In summary, the mapping function at each time step utilizes the network evolution information to explore the temporal development mechanisms of the network.

PROPOSED MODEL

As illustrated in Fig.2, the running process of *DyCSC* mainly consists of three components: 1) *ClusterLP*, only used at time $t = 0$, obtaining the embedding vectors of nodes in the network and the specified number of cluster centroids; 2) **T**ime-Regularization **C**luster-**A**ware **L**ink formation **P**robability Module (*TCALP*), used at time $t > 0$, adding a temporal consistency constraint to obtain the embedding vector for each node; 3) Memory Storage Module, a memory network was used to store the similarity between the nodes at each moment, and then read out the corresponding memory when needed. We elaborate on the details of each respective module in the following paragraphs.

CALP

To obtain the representation vector of nodes, the network structures must be preserved. The first intuition is that the local structure, i.e. the local pairwise proximity between vertices, must remain preserved. For each pair of vertices linked by an edge (v_i, v_j), the weight on that edge, w_{ij}, indicates the *first-order proximity*[] between v_i and v_j. If no edge is observed between v_i and v_j, their *first-order proximity* is 0.

We will use the Euclidean distance between two vectors to calculate their *first-order proximity*,

$$\mathcal{D}_{ij} = \Omega\left(h_i, h_j\right) = \left\|\mathcal{H}_i - \mathcal{H}_j\right\|^2 = \sqrt{\sum_{l=1}^{d}\left(\mathcal{H}_i^l - \mathcal{H}_j^l\right)^2} \tag{1}$$

Then the max abs normalization is used for $\mathcal{D}$ to limit the values of each of its elements to between 0 and 1, and obviously, a small value of $\mathcal{D}_{ij}$ favors the formation of link between v_i and v_j.

$$\mathcal{D} = \frac{\mathcal{D}}{max\left(\mathcal{D}\right)} \tag{2}$$

However, in a real world information network, a pair of nodes on a missing link has a zero first-order proximity, even though they are intrinsically very similar to each other. Therefore, *first-order proximity* alone is not sufficient for preserving the network structures, and it is important to seek

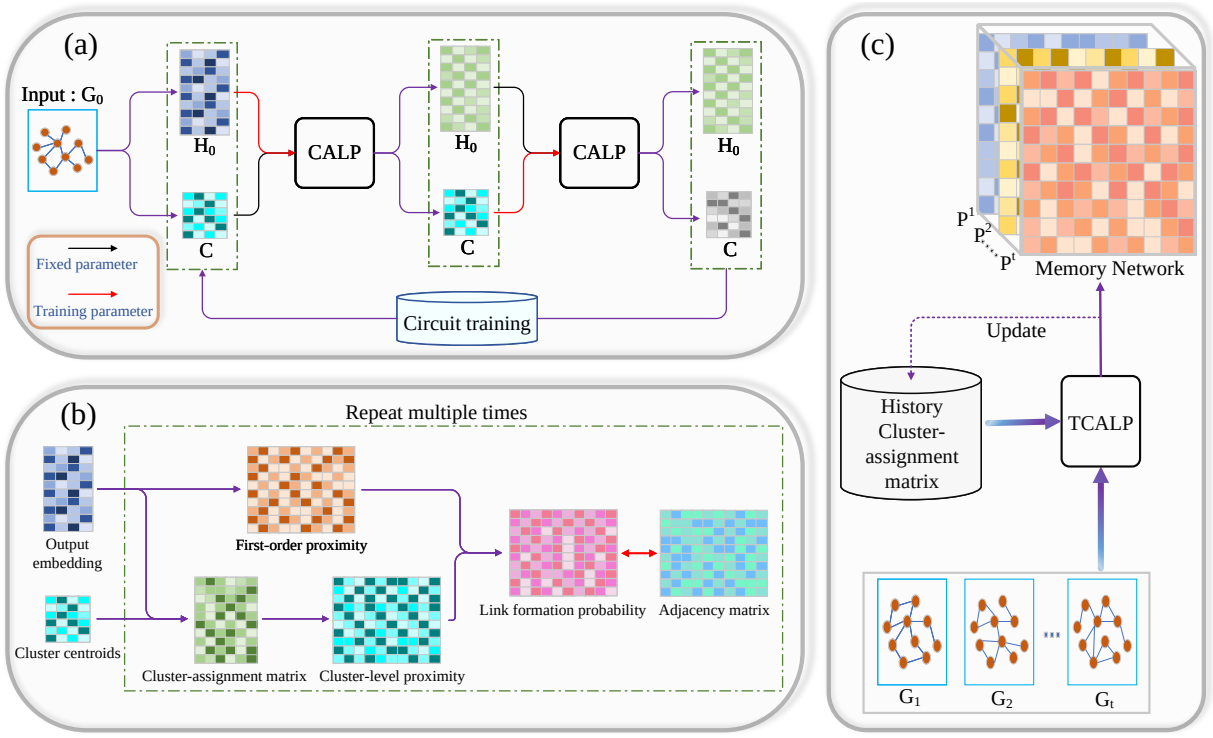

Figure 2: Overall operation process of the proposed *DyCSC* model. (a) shows the data flow of a *ClusterLP* unit;(b) is the illustration of the proposed **C**luster-**A**ware **L**ink formation **P**robability module (**CALP**) by simultaneously preserve the first-order proximity and cluster-level proximity between nodes.; (c) is a sketch illustrating the recurrent paradigm.

an alternative notion of proximity that addresses the problem of sparsity. A natural intuition is that vertices in the same cluster tend to be similar to each other. For example, in social networks, people in the same social group often have similar interests, thus becoming friends; in citation networks, a node (article) is more willing to quote articles in the same research field. We therefore define the *cluster-level proximity*, which complements the *first-order proximity* and preserves the network structure.

Definition. *(cluster-level proximity)* The *cluster-level proximity* between a pair of vertices (v_i, v_j) in a network is the similarity between their tendencies toward the clusters present in the network. Mathematically, if t_i and t_j represent the cluster assignment of nodes v_i and v_j respectively, then the *cluster-level proximity* between v_i and v_j is determined by the similarity between t_i and t_j. If v_i and v_j are in the same cluster, the *cluster-level similarity* between them is high, otherwise it will be close to 0.

To calculate a soft clustering assignment distribution of each node, we define the probability that node v_i belongs to cluster k as the tendency of vector h_i to cluster centroid u_k divided by the trend of h_i to all the clustering centroids, which can be expressed as mathematical formula:

$$t_{ik} = \Psi\left(\mathcal{H}_i, \mathcal{U}_k\right) = \left(1 + \frac{\left\|\mathcal{U}_k - \mathcal{H}_i\right\|^2}{n}\right)^{-1} \tag{3}$$

$$t_i = \Upsilon\left(t_{i1}, t_{i2}, \ldots, t_{i\mathcal{K}}\right) = \left[\frac{t_{i1}}{\sum_{l=1}^{\mathcal{K}} t_{il}}, \frac{t_{i2}}{\sum_{l=1}^{\mathcal{K}} t_{il}}, \ldots, \frac{t_{i\mathcal{K}}}{\sum_{l=1}^{\mathcal{K}} t_{il}}\right] \tag{4}$$

Our definition of clustering assignmentment for nodes is an improvement on the StudentâĂŹs t-distribution used in *DAEGC* [9], with only one more parameter n, so it does not break the advantages of being able to handle different scaled clusters and being computationally convenient. The hyperparameter n here is used to adjust the decay rate of cluster tendency, and the smaller n indicates that the cluster structure in the space is more obvious. We also define the cluster-assignment matrix as $T = [t_1, t_2, \ldots, t_N] \in \mathbb{R}^{N \times \mathcal{K}}$.

In order to capture the similarity between nodes v_i and v_j from a macroscopic perspective, we use cosine similarity to calculate the *cluster-level proximity* $\mathcal{C}_{ij}$ using the cluster assignmentment vectors t_i and t_j.

$$\mathcal{C}_{ij} = \frac{t_i \cdot t_j}{\left\|t_i\right\|^2 \cdot \left\|t_j\right\|^2} = \frac{\sum_{k=1}^{\mathcal{K}} t_{ik} \times t_{jk}}{\sqrt{\sum_{k=1}^{\mathcal{K}} \left(t_{ik}\right)^2} \times \sqrt{\sum_{k=1}^{\mathcal{K}} \left(t_{jk}\right)^2}} \tag{5}$$

The definition shows that the closer $\mathcal{C}_{ij}$ is to 1, indicating that vectors t_i and t_j are more similar, otherwise the similarity is smaller.

According to the previous analysis, the probability of forming a link between two nodes is proportional to their

cluster-level proximity, and inversely proportional to the *first-order proximity* between them, which can be expressed in a formula.

$$\mathcal{P} \propto \frac{\mathcal{C}}{\mathcal{D}} \tag{6}$$

There are many mathematical tools for modeling such relationships, including the widely used sigmoid function, and we have chosen a simple power function here due to its computationally simple and excellent convergence effect:

$$\mathcal{P}_{ij} = \Lambda\left(\mathcal{D}_{ij}, \mathcal{C}_{ij}\right) = \exp\left(-\beta \frac{\mathcal{D}_{ij}}{\mathcal{C}_{ij}}\right) \tag{7}$$

ClusterLP

We assume that the number of clusters $\mathcal{K}$ in the network is already known (as a hyperparameter of the model), *ClusterLP* will randomly assign a representation vector h_i to each node v_i in the network and $u_j \in \mathbb{R}^d$ to the centroid of each cluster j at the initial moment. *ClusterLP* will be divided in two stages to train the output embedding matrix $\mathcal{H} \in \mathbb{R}^{N \times d}$ and the cluster centroid matrix $\mathcal{U} \in \mathbb{R}^{\mathcal{K} \times d}$ by using *CALP*, respectively. In the first stage, *ClusterLP* takes $\mathcal{U}$ as a fixed parameter to calculate the probability of forming a link between each node pair to obtain the predicted network adjacency matrix $\mathcal{P}$. The position of each node in the representation space is adjusted through backpropagation error by comparison $\mathcal{P}_{train} = \{\mathcal{P}_{ij} \mid e_{ij} \in \mathcal{E}_{train}\}$ with $\mathcal{A}_{train} = \{\mathcal{A}_{ij} \mid e_{ij} \in \mathcal{E}_{train}\}$. Here, $\mathcal{E}_{train}$ represents the real links used for training. Similarly, $\mathcal{H}$ is used as a fixed parameter to update $\mathcal{U}$ in the second phase. $\mathcal{U}$ and $\mathcal{H}$ adjusted after the above two stages can be used as the initial state of the next loop, and after multiple loop updates, *ClusterLP* will get stable $\mathcal{U}$ and $\mathcal{H}$ that fully capture the node relationships in the network.

TCALP

To maximize the satisfaction of hypothesis 3, on the basis of *CALP*, we add a time constraint, that is, the tendency of the same node to various clusters should be not much different at the adjacent time.

In order to obtain the node embedding $\mathbf{H}^t$ ($t > 1$), its initial value is set to the stable node embedding obtained at the previous time($\mathbf{H}^{t-1}$). Note that $\mathcal{U}$ is used as a fixed parameter at this time and does not need to be trained.

We jointly optimize the reconstruction loss which can be achieved by minimizing the differences between $\mathbf{P}^t$ and $\mathcal{A}^t$ and clustering changing which is defined as the difference between $\mathbf{T}^t$ and $\mathbf{T}^{t-1}$, and thus define our total objective function as:

$$\mathcal{L}_{nodes} = \left\|\mathbf{P}^t - \mathcal{A}^t\right\| + \eta \left\|\mathbf{T}^t - \mathbf{T}^{t-1}\right\| \tag{8}$$

Memory Storage Module

The last hypothesis is the basis for the predictive validity of all time-series models, namely that changes in dynamic samples are subject to some regularity. Historical information plays an indispensable role in temporal graph modeling since it facilitates the model to learn the evolving patterns and regularities. Although the latest link formation probability $\mathbf{P}^{t-1}$ obtained by *ClusterLP* already carries historical information before time t, some discriminative contents may still be under-emphasized due to the monotonic mechanism of RNNs that temporal dependencies are decreased along the time span[6].

One of the major innovations of *DyCSC* is that, unlike other models storing hidden states obtained by recurrent neural networks (e.g., *HTGN*[11]) or other methods (e.g., *VGRNN*), *DyCSC* will directly use the probability of forming links between nodes at each moment. Inspired by [1], our proposed *DyCSC* maintains a memory $\mathbf{M} \in \mathbb{R}^{N \times N \times (T-1)}$ to store the historical states of the previous period and the definition of historical information used to predict the network state at time t is extended from the state $\mathbf{P}^{t-1}$ of the latest snapshot to the latest w snapshots $\mathbf{P}^t_{Memory} = \left\{\mathbf{P}^{t-w}, \ldots, \mathbf{P}^{t-2}, \mathbf{P}^{t-1}\right\}$, attending on multiple historical latent states to get a more informative hidden state.

Overall Model Training

In the dynamic graph embedding literature, the term *link prediction* has been used with different definitions. While some of the previous works focused on *link prediction* in a transductive setting and others proposed inductive models, our models are capable of working in both settings. We evaluate our proposed models on three different *link prediction* tasks that have been widely used in the dynamic graph representation learning studies. More specifically, given partially observed snapshots of a dynamic graph $\mathcal{G}$, dynamic *link prediction* problems are defined as follows: 1) dynamic link detection, i.e. detect unobserved edges in $\mathcal{A}^t$; 2) dynamic link prediction, i.e. predict edges in $\mathcal{A}^{t+1}$; 3) dynamic new link prediction, i.e. predict edges in $\mathcal{A}^{t+1}$ that are not in $\mathcal{A}^t$.

Dynamic link detection. When predicting the network topology $\mathcal{A}^t$ at the next moment, if part of the information in $\mathcal{A}^t$ is already known, we can first embed the nodes in $\mathcal{A}^t$ to obtain the approximate structural similarity between nodes $\mathbf{P}_{Compute}$, and then combine it with the information read from the memory network $\mathbf{P}^t_{Memory}$ to obtain the complete structural information. Finally, the multilayer neural network is used to assign different weights to the memory at different moments, thus obtaining the link formation probability $\mathbf{P}^t$. Fig.3 is a visualization of the above process.

$$\begin{aligned}\mathcal{L} = &\left\|\mathbf{MLP}\left(\mathbf{P}^t_{Memory} \oplus \mathbf{P}_{Compute}\right) - \mathcal{A}^t\right\| \\ &+ \eta \left\|\mathbf{T}^t - \mathbf{T}^{t-1}\right\|\end{aligned} \tag{9}$$

Dynamic (new) link detection. When the topology of network at the next moment $t+1$ is completely unknown, the only information we can use is the structural similarity between nodes in a previous period of time $\mathbf{M}$. At this time, the existing time series prediction model such as *LSTM* can take $\mathbf{M}$ as the input for prediction. In this paper, we will take the most simple and intuitive time series method to obtain $\mathbf{P}^{t+1}$. Specifically, we input $\mathbf{P}^t_{Memory}$ into a single-layer preceptron to predict $\mathbf{P}^t$, then adjust the weight of the perceptron according to the error between them, and finally in-

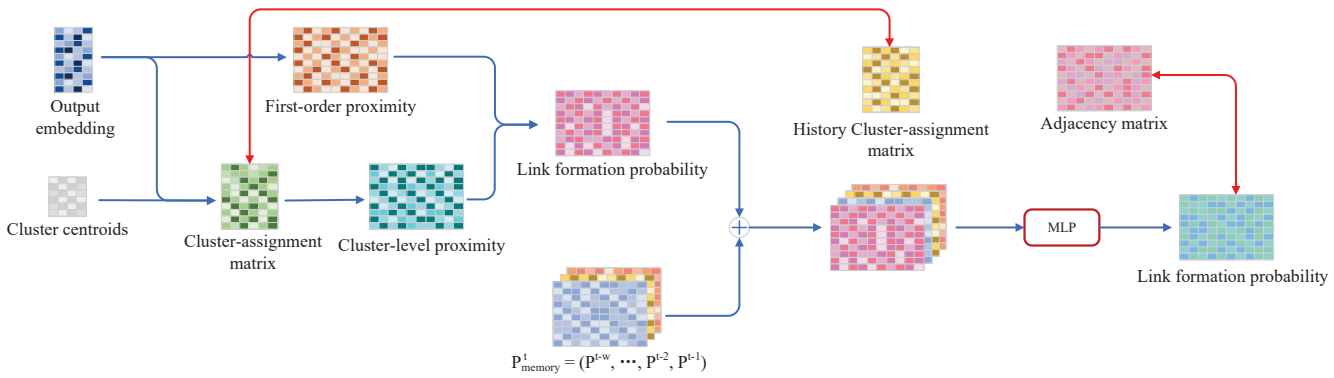

Figure 3: Schematic representation of the dynamic link detection using *DyCSC*.

Table 1: Datasets

Metrics	Enron	COLAB	Facebook
Number of Snapshots	11	10	9
Test Snapshots	3	3	3
Number of Nodes	184	315	663
Number of Edges	115-266	165-308	844-1068
Average Density	0.01284	0.00514	0.00591

put $\mathbf{P}^{t+1}_{Memory}$ into the perceptron to obtain the prediction results of the network topology $\mathcal{A}^{t+1}$.

EXPERIMENTS AND ANALYSIS

In this section, we conduct extensive experiments with the aim of answering the following research questions (RQs):

- **RQ1**. How does *DyCSC* perform?
- **RQ2**. What is the mechanism by which *DyCSC* can capture the dynamic changing processes of a temporal network, i.e., What does the time constraint bring?
- **RQ3**. What is the default value should be set for each hyperparameter in *DyCSC*?

Evaluation tasks

As was done by *VGRNN*, we conduct two different benchmarking tests on three real-world dynamic graphs as described in Table 1 to compare *DyCSC* with other temporal link prediction methods: inductive dynamic link detection and transductive dynamic link prediction.

Experimental setups

For performance comparison, we evaluate different methods based on their ability to correctly classify true and false edges. For dynamic link detection problem, we randomly remove 5% and 10% of all edges at each time for validation and test sets, respectively. We also randomly select the equal number of non-links as validation and test sets to compute average precision (AP) and area under the ROC curve (AUC) scores. For dynamic (new) link prediction, all (new) edges are set to be true edges and the same number of non-links are randomly selected to compute AP and AUC scores. In all of our experiments, we test the model on the last three snapshots of dynamic graphs while learning the parameters of the models based on the rest of the snapshots. For the datasets without node attributes, the identity matrix $\mathcal{I} \in \mathbb{R}^{|\mathcal{V}|\times|\mathcal{V}|}$ is used as the initial feature input for all models at time t.

Baseline Tools

We compared ClusterLP with state-of-the-art unsupervised graph representation learning models:

- *VGAE*[5] is a variational graph autoencoder approach for graph embedding with both topological and content information.
- *DynGraph2Vec*[2] is a model which passes adjacency vectors into an multilayer perceptron (MLP) and an RNN to capture graph dynamics using traditional deep learning techniques. The DynAE variant passes adjacency vectors through a deep autoencoder architecture; the DynRNN variant passes them through a recurrent neural network; and DynAERNN passes the output of deep autoencoders to an RNN to generate node embeddings.
- *Evolving GCN*[7] is a GCN whose parameters are passed through an LSTM or GRU at each timestep. In the EGCN-O variant, the GCN parameters are the input and output of an LSTM; in the EGCN-H variant, the GCN parameters are used as the hidden states of a GRU, which takes the previous embedding as input.
- *VGRNN*[3] is a hierarchical variational model that introduces additional latent random variables to jointly model the hidden states of a graph recurrent neural network (GRNN) to capture both topology and node attribute changes in dynamic graphs.
- *SGRNN*[10] also applies stochastic latent variables to simultaneously capture the evolution in node attributes and topology like *VGRNN*, with the difference being that *SGRNN* separates deterministic states from stochastic states in the iterative process to suppress mutual interference.
- *EULER*[4] is a general-purpose framework which consists of a model-agnostic graph neural network stacked

Table 2: Comparison of *DyCSC* to related works on dynamic link detection

Metrics	Methods	Enron	COLAB	Facebook
AUC	*VGAE*	88.26 ± 1.33	70.49 ± 6.46	80.37 ± 0.12
	DynAE	84.06 ± 3.30	66.83 ± 2.62	60.71 ± 1.05
	DynRNN	77.74 ± 5.31	68.01 ± 5.50	69.77 ± 2.01
	DynAERNN	91.71 ± 0.94	77.38 ± 3.84	81.71 ± 1.51
	EGCN-O	93.07 ± 0.77	90.77 ± 0.39	86.91 ± 0.51
	EGCN-H	92.29 ± 0.66	87.47 ± 0.91	85.95 ± 0.95
	VGRNN	94.41 ± 0.73	88.67 ± 1.57	88.00 ± 0.57
	SI-VGRNN	95.03 ± 1.07	89.15 ± 1.31	88.12 ± 0.83
	SGRNN	96.81 ± 0.43	89.66 ± 0.48	89.34 ± 0.23
	SI-SGRNN	$\mathbf{97.63 \pm 0.98}$	89.96 ± 1.27	89.31 ± 0.71
	EULER	97.34 ± 0.41	91.89 ± 0.76	92.20 ± 0.56
	DyCSC	97.39 ± 0.28	$\mathbf{92.71 \pm 0.57}$	$\mathbf{93.55 \pm 0.41}$
	DyCSC-T	87.12 ± 0.45	88.88 ± 0.26	91.59 ± 0.33
AP	*VGAE*	89.95 ± 1.45	73.08 ± 5.70	79.80 ± 0.22
	DynAE	86.30 ± 2.43	67.92 ± 2.43	60.83 ± 0.94
	DynRNN	81.85 ± 4.44	73.12 ± 3.15	70.63 ± 1.75
	DynAERNN	93.16 ± 0.88	83.02 ± 2.59	83.36 ± 1.83
	EGCN-O	92.56 ± 0.99	91.41 ± 0.33	84.88 ± 0.52
	EGCN-H	92.56 ± 0.72	88.00 ± 0.85	82.56 ± 0.91
	VGRNN	95.17 ± 0.41	89.74 ± 1.31	87.32 ± 0.60
	SI-VGRNN	96.31 ± 0.72	89.90 ± 1.06	87.69 ± 0.92
	SGRNN	97.15 ± 0.24	91.68 ± 0.41	89.98 ± 0.21
	SI-SGRNN	$\mathbf{97.40 \pm 0.91}$	92.03 ± 0.98	90.03 ± 0.42
	EULER	97.06 ± 0.48	92.85 ± 0.88	91.74 ± 0.71
	DyCSC	97.18 ± 0.35	$\mathbf{94.79 \pm 0.62}$	$\mathbf{93.94 \pm 0.33}$
	DyCSC-T	90.13 ± 0.22	91.64 ± 0.17	91.81 ± 0.28

upon a model-agnostic sequence encoding layer such as a recurrent neural network.

Experimental Results (RQ1)

We repeat each experiment 10 times and report the average value with the standard deviation on the test sets in Table 2 and Table 3, where the best results are in bold and enlarged, the second-best results are only in enlarged for each dataset. In the following, we discuss the results on dynamic link detection and (new) link prediction, respectively.

Dynamic Link Detection Table 2 summarizes the results for inductive link detection in different datasets and it is observed that *DyCSC* consistently maintained in the top two in the competing methods for this task across all three datasets, demonstrating the effectiveness of the proposed method.

- The prediction performance of the static graph embedding method *VGAE* is worse than most temporal network methods, suggesting that considering the varying patterns can help predict the structure.
- In tests where *DyCSC* does not outperform the state-of-the-art methods, the gap with the best model is not very obvious and even negligible, despite *DyCSC* having more stable performance, fewer parameters and faster prediction speed.
- *DyCSC* achieved remarkable success on COLAB and Facebook networks, pushing the prediction accuracy for them to a whole new height. Observation table 1 shows that the average density of the two networks is very small, indicating that *DyCSC* is more able to characterize the sparse network than the other models.

Dynamic (New) Link Prediction The prior construction based on previous time steps naturally allows *DyCSC* to predict links in the future, but note that static methods are not applicable to these tasks as the sequential order is omitted in the learning procedure of a static method, and *VGAE* is thus not evaluated. Table 3 shows the results for link prediction and new link prediction. The obvious conclusion is that the simplistic *DyCSC* model outperforms the more modern ones in almost every test. Specifically, we notice that the performance of each method drops by different degrees compared to the corresponding link detection task, while our *DyCSC* model produces more consistent results. For instance, the performance of the baselines degrades dramatically on COLAB (e.g., the best, *EULER* drops from 91.89% to 86.54% in AUC), but *DyCSC* only declines about 2%, which shows that *DyCSC* has strenger inductive ability.

Ablation Study (RQ2)

We further conduct an ablation study to validate the effectiveness of the time constraint of *DyCSC*, and name this variant as *DyCSC-T*. There is no restriction on cluster consistency in *DyCSC-T*, where the model is trained only by minimizing the loss between the inter-node link formation probability and the true topology, i.e.,

$$\mathcal{L}_{nodes} = \left\| \mathbf{P}^t - \mathcal{A}^t \right\| \tag{10}$$

$$\mathcal{L} = \left\| \mathbf{MLP}\left(\mathbf{P}_{Memory} \oplus \mathbf{P}_{Compute}\right) - \mathcal{A}^t \right\| \tag{11}$$

As observed from Table 2 and 3 that removing cluster smoothing constraint will cause severe performance degradation, which highlights the importance of this time consistency for capturing the changing trends in the network dynamics.

Parameter Analysis (RQ3)

There are four key hyperparameters in *DyCSC*: number of clusters $\mathbf{K}$, embedding dimension $\mathbf{d}$, length of memory w, and the importance of time constraint η. Among them, the default settings for $\mathbf{K}$ and $\mathbf{d}$ are available as suggested in the *ClusterLP* paper, i.e., $\mathbf{K} = 12$, $\mathbf{d} = 8$, $\beta = 4.5$.

Deeper insights on w. In the experiments on the above three tasks, models which process graph embeddings using a temporal prediction component(e.g., RNN and the Memory Storage Module used in *DyCSC*) were significantly better than DynAE which does not. This component enables temporal attributes of the data to be carried over from previous time steps. If a new edge has been seen in the distant past, or a pattern that indicates a new edge is likely to appear has previously been observed, this history is carried over by the component into future embeddings. Therefore, generally speaking, the larger the value of w, the more powerful it can comprehensively grasp the change process of the network topology, so the better prediction effect can be obtained. In the above experiments, we set w to T-3 for the link detection task, and w to T-4 for the link prediction task (Remove the last 3 test snapshots).

Impact of the parameter η. The parameter η determines the importance of protecting the cluster structure when node

Table 3: Comparison of *DyCSC* to related works on dynamic (new) link prediction

Metrics	Methods	dynamic link prediction			dynamic new link prediction		
		Enron	COLAB	Facebook	Enron	COLAB	Facebook
AUC	*DynAE*	74.22 ± 0.74	63.14 ± 1.30	56.06 ± 0.29	66.10 ± 0.71	58.14 ± 1.16	54.62 ± 0.22
	DynRNN	86.41 ± 1.36	75.70 ± 1.09	73.18 ± 0.60	83.20 ± 1.01	71.71 ± 0.73	73.32 ± 0.60
	DynAERNN	87.43 ± 1.19	76.06 ± 1.08	76.02 ± 0.88	83.77 ± 1.65	71.99 ± 1.04	76.35 ± 0.50
	EGCN-O	84.28 ± 0.87	78.63 ± 2.14	77.31 ± 0.58	84.42 ± 0.82	79.06 ± 1.60	75.95 ± 1.15
	EGCN-H	88.29 ± 0.87	80.80 ± 0.95	75.88 ± 0.32	87.00 ± 0.85	78.47 ± 1.27	74.85 ± 0.98
	VGRNN	93.10 ± 0.57	85.95 ± 0.49	89.47 ± 0.37	88.43 ± 0.75	77.09 ± 0.23	87.20 ± 0.43
	SI-VGRNN	93.93 ± 1.03	85.45 ± 0.91	90.94 ± 0.37	88.60 ± 0.95	77.95 ± 0.41	87.74 ± 0.53
	SGRNN	94.35 ± 0.37	88.67 ± 0.43	90.12 ± 0.23	90.38 ± 0.59	81.49 ± 0.32	87.71 ± 0.49
	SI-SGRNN	94.50 ± 0.98	89.02 ± 1.03	90.98 ± 0.61	90.46 ± 0.98	**82.04 ± 0.53**	88.02 ± 0.57
	EULER	93.15 ± 0.42	86.54 ± 0.20	90.88 ± 0.12	87.92 ± 0.64	78.39 ± 0.68	89.02 ± 0.09
	DyCSC	**94.85 ± 0.15**	**89.27 ± 0.26**	**92.93 ± 0.11**	**91.24 ± 0.28**	79.76 ± 0.17	**89.63 ± 0.23**
	DyCSC-T	93.86 ± 0.12	88.45 ± 0.21	90.50 ± 0.37	89.74 ± 0.25	79.36 ± 0.37	88.10 ± 0.18
AP	*DynAE*	76.00 ± 0.77	64.02 ± 1.08	56.04 ± 0.37	66.50 ± 1.12	58.82 ± 1.06	54.57 ± 0.20
	DynRNN	85.61 ± 1.46	78.95 ± 1.55	75.88 ± 0.42	80.96 ± 1.37	75.34 ± 0.67	75.52 ± 0.50
	DynAERNN	89.37 ± 1.17	81.84 ± 0.89	78.55 ± 0.73	85.16 ± 1.04	77.68 ± 0.66	78.70 ± 0.44
	EGCN-O	86.55 ± 1.57	81.43 ± 1.69	76.13 ± 0.52	86.92 ± 0.39	81.36 ± 0.85	73.66 ± 1.25
	EGCN-H	89.33 ± 1.25	83.87 ± 0.83	74.34 ± 0.53	86.46 ± 1.42	79.11 ± 2.26	73.43 ± 1.38
	VGRNN	93.29 ± 0.69	87.77 ± 0.79	89.04 ± 0.33	87.57 ± 0.57	79.63 ± 0.94	86.30 ± 0.29
	SI-VGRNN	94.44 ± 0.85	88.36 ± 0.73	90.19 ± 0.27	87.88 ± 0.84	81.26 ± 0.38	86.72 ± 0.54
	SGRNN	94.58 ± 0.24	89.92 ± 0.57	89.37 ± 0.36	90.19 ± 0.32	82.81 ± 0.40	86.98 ± 0.34
	SI-SGRNN	**94.96 ± 0.91**	90.87 ± 0.80	90.03 ± 0.42	**90.21 ± 0.91**	**83.79 ± 0.72**	87.07 ± 0.58
	EULER	94.10 ± 0.32	89.03 ± 0.08	89.98 ± 0.19	88.49 ± 0.55	81.34 ± 0.62	87.54 ± 0.11
	DyCSC	94.62 ± 0.24	**91.78 ± 0.18**	**92.56 ± 0.17**	89.32 ± 0.33	82.15 ± 0.25	**88.69 ± 0.21**
	DyCSC-T	89.74 ± 0.25	79.36 ± 0.37	88.10 ± 0.18	88.11 ± 0.16	81.93 ± 0.22	87.17 ± 0.28

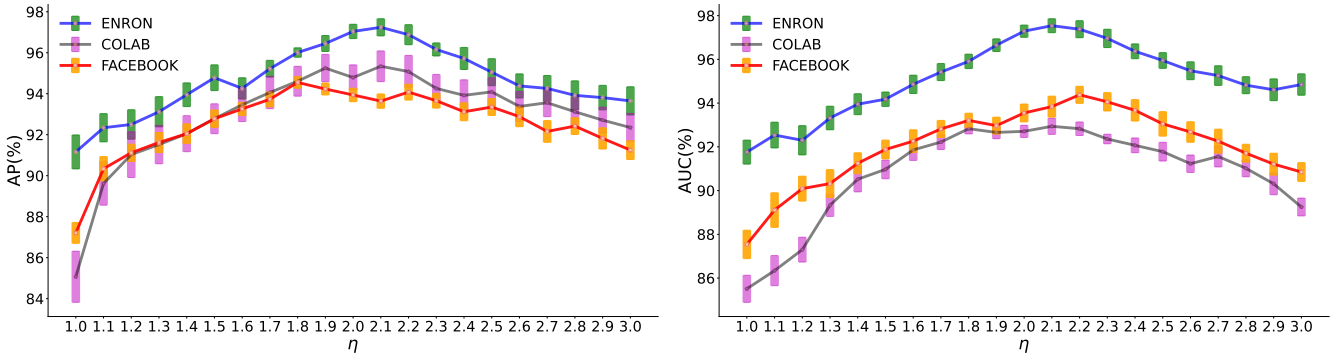

Figure 4: The changes of two evaluation metrics on the link detection task w.r.t. different values of η.

embedding is carried out in the network $\mathcal{G}_t$ ($t > 1$). Obviously, η needs to be set to a large value when the network cluster structure changes little at adjacent moments, forcing the model to capture and utilize this key information; similarly, when the cluster of the network changes dramatically, the value of η needs to be set relatively small to avoid distorting the reality. As can be seen from figure 4 that with the increase of η from 1.0 to 3.0, the values of AP and AUC are rising first and then falling when η exceeds about 2.0. Our multiple experiments show that it is generally very effective to set the initial value of η to 2.0, and that the value of η is also always set to 2.0 in all the experiments we constructed.

Conclusion

In summary, *DyCSC* follows the general practice of processing time series, i.e., storing the network state at each time point and reading out the required information when needed to predict the state at the next moment. Compared with other existing models, the biggest innovation point of *DyCSC* is to explicitly propose to combine the cluster structure changes of temporal networks to obtain the node representation vectors that can accurately reflect the process of network evolution. Specifically, a completely new time-constraint and memory storage component are proposed to ensure the excellent performance of *DyCSC*.

References

[1] Cui, S. W.; and Huang, L. W. 2019. A hierarchical contextual attention-based network for sequential recommendation. *Neurocomputing*, 358: 141–149.

[2] Goyal, S. R. C.; and Canedo. 2020. dyngraph2vec: Capturing network dynamics using dynamic graph representation learning. *Knowledge-Based Systems*, 187: 104816.

[3] Hajiramezanali, A. H.; Narayanan, N. D.; and Zhou, X. Q. 2019. Variational graph recurrent neural networks. In *Proceedings of the 24th Conference and Workshop on Neural Information Processing Systems*, 10701–10711.

[4] King, H. H. 2022. Euler: Detecting Network Lateral Movement via Scalable Temporal Graph Link Prediction. In *Proceedings of the Network and Distributed System Security Symposium*.

[5] Kipf, M. W. 2016. Variational graph auto-encoders. In *Proceedings of the 21th Conference and Workshop on Neural Information Processing Systems*.

[6] Liu, G. W.; Hu, L. D.; and Kot. 2017. Global context-aware attention lstm networks for 3d action recognition. In *Proceedings of the Conference on Computer Vision and Pattern Recognition*, 1647–1656.

[7] Pareja, G. D.; Chen, T. M.; Suzumura, H. K.; and Kaler, C. E. L. 2020. EvolveGCN: Evolving Graph Convolutional Networks for Dynamic Graphs. In *Proceedings of the 34th National Conference on Artificial Intelligence*, 5363–5370. AAAI Press.

[8] Skarding, B. G.; and Musial. 2020. Foundations and modelling of dynamic networks using Dynamic Graph Neural Networks: A survey. arXiv:2005.07496.

[9] Wang, S. P.; Hu, G. L.; and Jiang, C. Z. 2019. Attributed graph clustering: A deep attentional embedding approach. In *Proceedings of the Eighth International Joint Conference on Artificial Intelligence*, 3670–3676. IJCAI Organization.

[10] Yan, H. Z.; and Li, Y. X. 2022. Stochastic Graph Recurrent Neural Network. *Neurocomputing*, 500: 1003–1015.

[11] Yang, M. Z.; Kalander, Z. H.; and King. 2021. Discrete-time temporal network embedding via implicit hierarchical learning in hyperbolic space. In *Proceedings of the 27th ACM SIGKDD Conference on Knowledge Discovery & Data Mining*, 1975–1985.

[12] Zhou, Y. Y.; Ren, F. W.; and Zhuang. 2018. Dynamic Network Embedding by Modeling Triadic Closure Process. In *Proceedings of the Thirty-Second National Conference on Artificial Intelligence*. AAAI Press.